

MICROCOMPUTER COMPUTATION OF NATURAL CONVECTION HEAT TRANSFER FROM ISOTHERMAL SPHERES INTO AIR FOR RAYLEIGH NUMBERS FROM 1.5 TO 10⁷

C. C. Lo Choy, Graduate Research Assistant and M. M. Yovanovich,
 Professor and Director
 Microelectronics Heat Transfer Laboratory
 Department of Mechanical Engineering
 University of Waterloo
 Waterloo, Ontario, Canada

ABSTRACT

The integral method is employed for fast microcomputer computation of natural convection heat transfer from isothermal spheres in air. The governing equations are the boundary layer equations, expressed in spherical coordinates to account for curvature effects. The equations are solved by using the integral method in conjunction with assumed velocity and temperature profiles. On average, solution times for computing the surface-mean Nusselt number are about 8 and 12 minutes of an IBM PC-AT and IBM PC-XT computational time per solution respectively. Surface-mean Nusselt numbers are computed for Rayleigh numbers ranging between 1.5 and 10⁷. Comparison of the results of the present study with the available data from different sources shows good agreement over a wide range of Rayleigh numbers.

NOMENCLATURE

C_p specific heat capacity [J/kg·K]
 D diameter of sphere [m]
 $D_\Lambda(\theta)$ function of θ in Eq. (13)
 $\mathcal{F}(\theta)$ function of θ in Eq. (14)
 g gravitational acceleration [m/sec²]
 g_θ tangential gravitational component [m/sec²]
 Gr_D Grashof number, $g\beta(\bar{T}_w - \bar{T}_\infty)D^3/\nu^2$
 $I_s(\theta)$ function of θ in Eq. (14)
 k thermal conductivity [W/m²·K]
 $Nu_D(\theta)$ local Nusselt number
 \overline{Nu}_D surface-mean Nusselt number
 \overline{Nu}_D^∞ diffusive surface-mean Nusselt number
 Pr Prandtl number, ν/α
 \bar{r} radial distance [m]

\bar{r}_w radius of sphere [m]
 r dimensionless radial distance
 \bar{r}, θ, φ spherical coordinates
 Ra_D Rayleigh number, $g\beta(\bar{T}_w - \bar{T}_\infty)D^3/\nu\alpha$
 rms root mean square
 \bar{T} temperature of fluid [K]
 T dimensionless temperature
 T_g function of δ_t in Eq. (15)
 T_n function of δ_t in Eq. (15)
 \bar{T}_w wall temperature [K]
 \bar{T}_∞ ambient temperature [K]
 \bar{u} tangential velocity [m/sec]
 u dimensionless tangential velocity, $\bar{u}D/\alpha$
 \bar{v} radial velocity [m/sec]
 v dimensionless radial velocity, $\bar{v}D/\alpha$
 v_{ref} reference velocity, α/D [m/sec]
 $W_c(\theta)$ function of θ in Eq. (16)
 $Z_c(\theta)$ function of θ in Eq. (16)

Greek Symbols

ρ fluid density [kg/m³]
 α thermal diffusivity of fluid, $k/(\rho C_p)$ [m²/sec]
 β thermal expansion coefficient [K⁻¹]
 $\bar{\delta}_m$ hydraulic boundary layer thickness [m]
 $\bar{\delta}_t$ thermal boundary layer thickness [m]
 δ dimensionless hydraulic boundary layer thickness
 δ_t dimensionless thermal boundary layer thickness
 ν kinematic viscosity [m²/sec]
 η_m, η_t normalized boundary layer thickness
 $\Lambda(\theta)$ function of θ in Eq. (13)
 δ_0 dimensionless hydraulic boundary layer at $\theta = 0$
 $\delta_{t,0}$ dimensionless thermal boundary layer at $\theta = 0$

Subscripts

D characteristic body length based on sphere diameter
 w wall conditions

INTRODUCTION

Due to the ubiquity of spherical configurations in many engineering applications such as in packed beds of spherical bodies for heat transfer, great efforts have been devoted in the past to natural convection heat transfer from isothermal spheres. The governing equations which are encountered in such problems are the continuity, momentum and energy. As will be seen in a subsequent section, these equations are complicated by being non-linear in nature. In natural convection, further complication arises due to the coupling of the momentum and energy equations. Because of the mathematical difficulties associated with these equations, their exact analytical solutions are not to be expected. In the heat transfer literature, the various approaches undertaken by different authors to obtain solutions of the governing equations for the case of natural convection heat transfer from isothermal spheres, can be classified into three main categories: (i) analytical methods, (ii) experimental techniques, and (iii) numerical methods.

Analytical investigations have mainly centered upon the two asymptotic solutions; the laminar boundary layer limit for $10^4 < Ra_D < 10^8$ (Merk and Prins, 1953 - 1954, Chiang and Tien, 1964) and the diffusive limit for $Ra_D < 10^{-4}$ (Yovanovich, 1987). However, many situations arise where solutions are required for Rayleigh numbers in the transition regime between the two asymptotes ($10^{-4} < Ra_D < 10^4$). Due to the complexity of the mathematical modelling of the heat transfer process in the transition regime, most of the heat transfer data available today in this range of Rayleigh numbers are furnished by experimental techniques (Kyte et al., 1953, Yuge, 1960, Amato and Tien, 1972, Chamberlain, 1983). In general, the experimental approach has the capability of supplying realistic heat transfer data; however, it is time consuming and expensive. Hossain and Gebhart (1970) employed an expansion technique to obtain values for the Nusselt number for isothermal spheres at low Grashof number ($0 < Gr_D < 1$) and Prandtl number around unity. This approach is complicated, involving the solution of the full momentum equations in spherical coordinates. In addition, their solutions were reported to be significantly lower than prior experimental data. Significant contributions to natural convection heat transfer have been made by Raithby and Hollands (1975), who developed an approximate method for predicting natural convection heat transfer from isothermal bodies of arbitrary shape, which include the spheres. This approximate method reduces the more complex natural convection problem into a simpler equivalent conduction problem, by surrounding the body with a stationary layer of fluid of variable thickness which offers the same thermal resistance as the original problem.

Analytical methods discussed above usually involve the introduction of simplifying assumptions to make the heat transfer problem more amenable to mathematical treatments. Numerical methods, on the other hand, require only a limited number of assumptions and can handle non-linearities encountered in heat transfer problems. In spite of this, very few numerical studies of natural convection heat transfer from isothermal spheres at low Rayleigh numbers exist in the literature. An early attempt was made by Geoola and Cornish (1981) to compute Nusselt number from an isothermal sphere at low Grashof number ($0.05 < Gr_D < 50$) and Prandtl number of

0.72 (air). The computational time for solutions at $Gr_D = 50$ and $Gr_D = 25$ were reported to be as long as 4 and 3 hours on a CDC6400 digital computer respectively. Moreover, the finite difference results of Geoola and Cornish were not in satisfactory agreement with experimental data. Recently, more satisfactory results were obtained by Farouk (1982), who tackled the same problem and obtained finite difference results for the surface-mean Nusselt numbers that are in good agreement with Yuge's empirical correlation (Yuge, 1960).

Numerical methods have limitations; among which the most common ones are the limited storage capacity and speed of the computer. In view of this, the integral method has long been utilized to obtain fast and reasonably accurate results for many natural convection problems, which would otherwise be difficult and expensive to handle. In the past, integral methods have been restricted to solutions of natural convection problems in the local body cartesian coordinate system (Merk and Prins, 1953 - 1954, Levy, 1955, Jaluria, 1980). Such coordinate system was reported to be insufficient for accurate results at low Rayleigh numbers, instead a coordinate system which is compatible to the body shape being analyzed should be used to account for the curvature effects at low Rayleigh numbers (Peterka and Richardson, 1969). The proper selection of the coordinate system is therefore essential in the formulation of integral methods for low Rayleigh numbers flow condition.

In the present study, the von Kármán integral method is employed to estimate natural convection heat transfer rates from isothermal spheres in air. It is common practice in the heat transfer literature to restrict the boundary layer theory and associated approximations to the laminar boundary layer regime. In this study, the application of the boundary layer theory is extended to the transition regime to obtain surface-mean Nusselt numbers over a wide range of Rayleigh numbers. The basic equations for the present study are therefore the boundary layer equations, expressed in spherical coordinates to account for curvature effects at low Rayleigh numbers. These equations are then solved by the von Kármán integral method in conjunction with assumed velocity and temperature profiles. The numerical aspects of the present study are performed on both an IBM PC-AT and IBM PC-XT and their respective computational time is examined. Finally, an assessment of the accuracy of the present study is obtained by comparing the computed surface-mean Nusselt numbers with the available heat transfer data from different sources.

THEORETICAL ANALYSIS

The body being analyzed is at a constant surface temperature \hat{T}_w and is immersed in an extensive, quiescent fluid of constant temperature \hat{T}_∞ . According to the Boussinesq approximation, the properties of the fluid surrounding the body are assumed constant, except the density variation which is accounted for in the buoyancy term only. Based on the boundary layer theory, the existence of hydraulic and thermal boundary layers are assumed around the body. The present problem is formulated in a spherical coordinate system $(\bar{r}, \theta, \varphi)$, where \bar{r} is the radial coordinate, θ is the angular coordinate in the direction of fluid flow and φ is the angle of rotation about the axis of revolution of the body (Fig. 1). The basic equations for the

present study are therefore the following boundary layer equations expressed in spherical coordinates (Hughes and Gaylord, 1964):

Continuity equation:

$$\frac{1}{\bar{r}} \frac{\partial \bar{u}}{\partial \theta} + \frac{\partial \bar{v}}{\partial \bar{r}} + \frac{\cot \theta}{\bar{r}} \bar{u} = 0 \quad (1)$$

θ -momentum equation:

$$\frac{\bar{u}}{\bar{r}} \frac{\partial \bar{u}}{\partial \theta} + \bar{v} \frac{\partial \bar{u}}{\partial \bar{r}} = \nu \frac{\partial^2 \bar{u}}{\partial \bar{r}^2} + g_\theta \beta (\bar{T} - \bar{T}_\infty) \quad (2)$$

Energy equation:

$$\bar{v} \frac{\partial \bar{T}}{\partial \bar{r}} + \frac{\bar{u}}{\bar{r}} \frac{\partial \bar{T}}{\partial \theta} = \alpha \frac{1}{\bar{r}^2} \frac{\partial}{\partial \bar{r}} \left\{ \bar{r}^2 \frac{\partial \bar{T}}{\partial \bar{r}} \right\} \quad (3)$$

where the tilde denotes a dimensional quantity, g_θ is the component of gravity in the θ -direction, \bar{v} and \bar{u} are the dimensional velocities in the \bar{r} and θ direction respectively, ν is the kinematic viscosity, β is the coefficient of thermal expansion, and α is the thermal diffusivity of the fluid. To non-dimensionalize the foregoing equations, the following dimensionless variables are introduced:

$$u = \frac{\bar{u}}{v_{ref}}, \quad v = \frac{\bar{v}}{v_{ref}}, \quad r = \frac{\bar{r} - \bar{r}_w}{D}, \quad T = \frac{\bar{T} - \bar{T}_\infty}{\bar{T}_w - \bar{T}_\infty} \quad (4)$$

where u , v and T are the dimensionless angular velocity, radial velocity and temperature respectively; $v_{ref} = \alpha/D$ is chosen as the reference velocity to eliminate the dependency of the energy equation on the Prandtl number, Pr . The temperature is in fact independent of Pr at sufficiently high Pr . Substituting these dimensionless variables into Eqs. (1) - (3) yields after simplifications:

$$\frac{1}{(r+1/2)} \frac{\partial u}{\partial \theta} + \frac{\partial v}{\partial r} + \frac{\cot \theta}{(r+1/2)} u = 0 \quad (5)$$

$$\frac{1}{Pr} \left\{ \frac{u}{(r+1/2)} \frac{\partial u}{\partial \theta} + v \frac{\partial u}{\partial r} \right\} = \frac{\partial^2 u}{\partial r^2} + Ra_D \sin \theta T \quad (6)$$

$$v \frac{\partial T}{\partial r} + \frac{u}{(r+1/2)} \frac{\partial T}{\partial \theta} = \frac{1}{(r+1/2)^2} \frac{\partial}{\partial r} \left\{ (r+1/2)^2 \frac{\partial T}{\partial r} \right\} \quad (7)$$

where $Ra_D = [g\beta(\bar{T}_w - \bar{T}_\infty)D^3/\alpha\nu]$ is the Rayleigh number based on the diameter of the sphere. The foregoing equations are mathematically more complex than the classical boundary layer formulation, where the equations are cast in local body cartesian coordinates. For this reason, solutions are not sought for Eqs. (5) - (7) in their original form. Instead, Eqs. (6) and (7) are integrated across the boundary layers with respect to the radial coordinate r to give the following momentum and energy integral equations:

$$\frac{1}{Pr \sin \theta} \frac{\partial}{\partial \theta} \left\{ \sin \theta \int_0^{\delta} \frac{u^2}{(r+1/2)} dr \right\} - Ra_D \sin \theta \int_0^{\delta_t} T dr = - \frac{\partial u}{\partial r} \Big|_{r=0} \quad (8)$$

$$\frac{1}{\sin \theta} \frac{\partial}{\partial \theta} \left\{ \sin \theta \int_0^{\delta} \frac{uT}{(r+1/2)} dr \right\} = \int_0^{\delta_t} \left\{ \frac{2}{(r+1/2)} \frac{\partial T}{\partial r} + \frac{\partial^2 T}{\partial r^2} \right\} dr \quad (9)$$

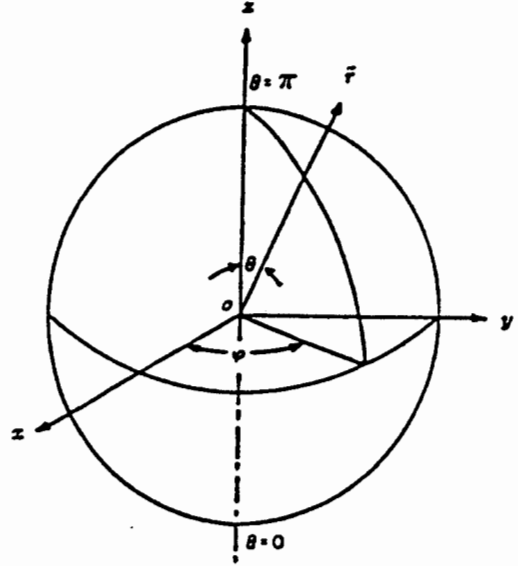


Figure 1: Spherical Polar Coordinate System (\bar{r}, θ, φ)

in which the dependency upon the radial velocity component v has been eliminated by means of the continuity equation, and $\delta = \bar{\delta}/D$ and $\delta_t = \bar{\delta}_t/D$ are the dimensionless hydraulic and thermal boundary layer thicknesses respectively. It is noteworthy of mentioning that Eq. (9) is only valid for $Pr < 1$, i.e when the thermal diffusivity is greater than the momentum diffusivity or when $\delta < \delta_t$. For $Pr > 1$ or when $\delta > \delta_t$, the upper limit of the first integral in Eq. (9) should be replaced by δ_t . In integral methods, the conservation of mass, momentum and energy are ascertained only on the average over a small control volume extending across the boundary layers. As a result of this, the velocity and temperature variations across the boundary layers have to be supplied externally by assuming velocity and temperature profiles that satisfy a few of the boundary conditions at the surface and the edge of the boundary layers. In this study, a fourth order polynomial in $\eta_m = r/\delta$ is chosen for the tangential velocity profile in such a way that it satisfies the following boundary conditions at the surface ($\eta_m = 0$) and at the edge of the hydraulic boundary layer ($\eta_m = 1$):

$$\left. \begin{aligned} u = 0, \text{ and } \frac{1}{\bar{r}^3} \frac{\partial^3 u}{\partial \eta_m^3} \Big|_{\eta_m=0} = -Ra_D \frac{\sin \theta}{\delta_t} \frac{\partial T}{\partial \eta_t} \Big|_{\eta_t=0} \text{ at } \eta_m = 0 \\ u = 0, \frac{\partial u}{\partial \eta_m} = 0, \text{ and } \frac{\partial^2 u}{\partial \eta_m^2} = 0 \text{ at } \eta_m = 1 \end{aligned} \right\} \quad (10)$$

where $\eta_m = r/\delta$ and $\eta_t = r/\delta_t$ are the normalized hydraulic and thermal boundary layer thickness respectively, and the second condition imposed on the velocity at the surface is derived by evaluating the derivative of Eq. (6) at $\eta_m = 0$. Using Eq. (10), the assumed velocity distribution profile can be derived and is given as:

$$u = -\frac{1}{6} Ra_D \sin \theta \frac{\delta^3}{\delta_t} \frac{\partial T}{\partial \eta_t} \Big|_{\eta_t=0} \left[\frac{1}{3} \eta_m - \eta_m^2 + \eta_m^3 - \frac{1}{3} \eta_m^4 \right] \quad (11)$$

To correct for the expected inaccuracies associated with the use of the boundary layer equations at low Rayleigh numbers, the

assumed temperature profile is taken as that corresponding to pure radial conduction; this profile is approached as $Ra_D \rightarrow 0$ and can be derived from Laplace's equation (1985). When expressed in terms of η_t , the assumed temperature profile can then be written as:

$$T(\eta_t, \theta) = \frac{1 - \eta_t}{2\delta_t \eta_t + 1} \quad (12)$$

and satisfies the two thermal boundary conditions $T = 1$ at $\eta_t = 0$ and $T = 0$ at $\eta_t = 1$. However, it does not satisfy the condition which arises in natural convection problems and which requires the temperature gradient to be negligible at $\eta_t = 1$, i.e. $\frac{\partial T}{\partial \eta_t} \Big|_{\eta_t=1} = 0$. Expressing the momentum and energy integral equations in terms of η_m and η_t , and substituting Eqs. (11) and (12) into the resulting equations yield the following set of linear ordinary differential equations, after some major mathematical manipulations:

$$\left[\frac{Ra_D \sin \theta}{18Pr} T_g^2 [\delta^\tau D_\Lambda(\theta) + 7\delta^6 \Lambda(\theta)] \right] \frac{d\delta}{d\theta} - \left[\frac{Ra_D \sin \theta}{9Pr} \delta^\tau \times \Lambda(\theta) \frac{T_g}{\delta_t^2} \right] \frac{d\delta_t}{d\theta} = -\frac{1}{18} \delta^2 T_g + T_n - \frac{Ra_D}{6Pr} \delta^\tau T_g^2 \Lambda(\theta) \cos \theta \quad (13)$$

and

$$\left[\delta_t (1 + 2\delta_t) \left[\frac{4}{\delta} + \frac{F(\theta)}{I_s(\theta)} \right] \right] \frac{d\delta}{d\theta} - \left[1 + \frac{W_e \delta}{I_s(\theta)} \left(\frac{1 + 2\delta_t}{\delta_t} \right) \right] \frac{d\delta_t}{d\theta} = \frac{3\delta_t}{(1 + 2\delta_t) Ra_D \sin \theta \delta^4 I_s(\theta)} - 2\delta_t (1 + 2\delta_t) \cot \theta \quad (14)$$

in which

$$T_g = 2 + \frac{1}{\delta_t} \quad \text{and} \quad T_n = \left(\frac{1}{2} + \frac{1}{4\delta_t} \right) \ln(2\delta_t + 1) - \frac{1}{2} \quad (15)$$

where $\Lambda(\theta)$ and $I_s(\theta)$ are functions of θ , obtained respectively from the evaluation of the first integrals in Eqs. (8) and (9) using the assumed velocity and temperature profiles. $D_\Lambda(\theta)$, and $F(\theta)$ are functions that result from the derivatives of $\Lambda(\theta)$ and $I_s(\theta)$ with respect to θ respectively. Finally, functions $Z_e(\theta)$ and $W_e(\theta)$ are related to $I_s(\theta)$, as given below:

$$I_s(\theta) = Z_e + \frac{\delta}{\delta_t} W_e \quad (16)$$

For brevity, detailed definitions of the foregoing functions will not be presented herein; however, the interested readers can consult the author's thesis (Lo Choy, 1988) for more information. The two dependent variables associated with Eqs. (13) and (14) are δ and δ_t , which can then be numerically solved simultaneously on a personal computer.

NUMERICAL ANALYSIS

Initial Conditions for δ and δ_t

Prior to the numerical solution of Eqs. (13) and (14), the initial conditions are required at the frontal stagnation point ($\theta = 0$). However, δ and δ_t at $\theta = 0$ are not known and have to be determined. By symmetry arguments, $\frac{d\delta}{d\theta} \Big|_{\theta=0}$ and $\frac{d\delta_t}{d\theta} \Big|_{\theta=0}$ in

Eqs. (13) and (14) can be set to zero, resulting in the following equations:

$$\frac{Ra_D}{6Pr} \left(\frac{1 + 2\delta_{t,0}}{\delta_{t,0}} \right)^2 \delta_0^\tau \Lambda + \frac{\delta_0^2}{18} \left(\frac{1 + 2\delta_{t,0}}{\delta_{t,0}} \right) - \left[\left(\frac{1}{2} + \frac{1}{4\delta_{t,0}} \right) \times \ln(2\delta_{t,0} + 1) - \frac{1}{2} \right] = 0 \quad (17)$$

and

$$\delta_{t,0}^3 (4Z_e) + 4\delta_{t,0}^2 (Z_e + W_e \delta_0) + \delta_{t,0} (Z_e + 4W_e \delta_0 - [3/(2Ra_D \delta_0^4)]) + W_e \delta_0 = 0 \quad (18)$$

where δ_0 and $\delta_{t,0}$ denote the values of δ and δ_t at $\theta = 0$ respectively and functions $\Lambda(\theta)$, $Z_e(\theta)$, $W_e(\theta)$ are evaluated at $\theta = 0$. Equations (17) and (18) are then simultaneously solved by an iterative technique, which involves the following steps:

- Guess an initial value for $\delta_{t,0}$, denoted by $\delta_{t,0}^0$
- Substitute $\delta_{t,0}^0$ into Eq. (17) and solve for δ_0 by a Newton-Raphson method.
- Substitute the calculated value of δ_0 into Eq. (18) and solve for an updated value for $\delta_{t,0}$, denoted by $\delta_{t,0}^n$.
- Replace the initial guess $\delta_{t,0}^0$ by $\delta_{t,0}^n$ and repeat steps (b) and (c)
- Stop iteration when the percentage difference between $\delta_{t,0}^n$ and $\delta_{t,0}^{n-1}$ is within a specified tolerance (TOL).

Computer Code

The results of the iterations are the values of δ_0 and $\delta_{t,0}$ which are then used to initiate the numerical solution of Eqs. (13) and (14) by means of a fourth order Runge-Kutta integral method (Cheney and Kincaid, 1985). The flow chart for the computer code is shown in Fig. 2. Once the local thermal boundary layer thickness is known, the local and surface-mean

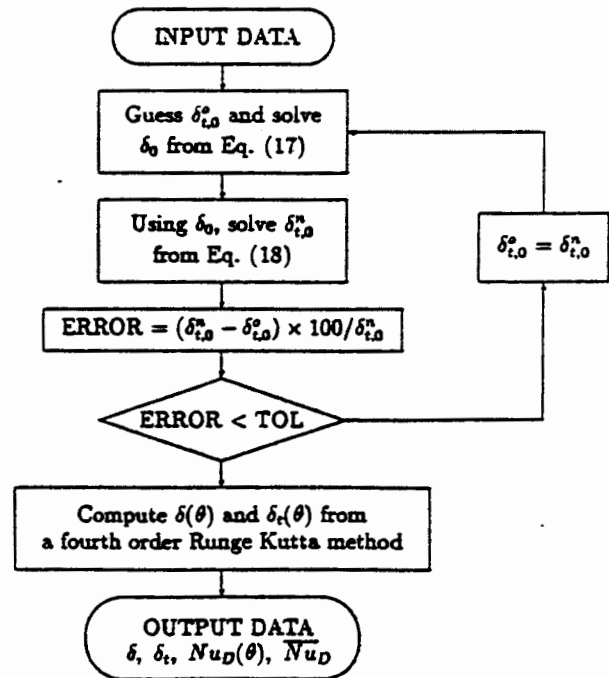


Figure 2: Flow chart for computer code

Nusselt number are determined from the following expressions:

$$Nu_D(\theta) = 2 + \frac{1}{\delta_t} \quad (19)$$

$$\overline{Nu}_D = 2 + \frac{1}{2} \int_0^\pi \frac{\sin \theta}{\delta_t} d\theta \quad (20)$$

It is interesting to note that Eqs. (19) and (20) for the local and surface-mean Nusselt numbers are composed of the linear superposition of the two asymptotes; the diffusive limit 2 and a second term which represents the laminar boundary layer limit. At low Rayleigh number where δ_t is large, the first term in the foregoing equations is predominant. However, at high Ra_D , δ_t is very small and consequently the Nusselt number is almost entirely dependent on the magnitude of the second term. The computer code developed for the numerical aspect of the present study is written in doubleprecision and consists of less than 650 line statements. No sophisticated solver is required in the computer program, as opposed to the finite difference scheme where solutions of the finite difference equations usually require special routines to keep the computer storage requirement and computational time to a minimum. Small fluctuations in the computed values of δ and δ_t were detected in the vicinity of the frontal stagnation point ($\theta < 3^\circ$) as Ra_D decreases. From a mathematical point of view, these fluctuations would not have a significant effect on \overline{Nu}_D due to the small surface area available for heat transfer in this region. However, due to the many numerical problems that may arise from these fluctuations or instabilities, great care was taken to eliminate or reduce them to a minimum by reducing the step size in the Runge-Kutta routine as Ra_D decreases.

RESULTS AND DISCUSSION

Surface-mean Nusselt numbers are computed for Rayleigh numbers in the range $1.5 \leq Ra_D \leq 10^7$. The computational time for solution is largest at low Rayleigh numbers, due to the smaller step sizes used in the computer code as the Rayleigh number decreases. The accuracy of the computed Nusselt number is found to be quite insensitive to the step size. The speed of convergence of the iterative scheme, used for solutions at the stagnation point, depends on the initial estimate for $\delta_{t,0}$. However, irrespective of the magnitude of the initial guess (as long as it is realistic), the iteration converges to the same value for $\delta_{t,0}$, thus leading to the computation of the same value for \overline{Nu}_D (Lo Choy, 1988). On average, the solution times for computing \overline{Nu}_D are about 12 and 8 minutes of IBM PC-XT and IBM PC-AT computational time per solution respectively. The present analysis therefore provides a remarkable improvement in the computational time and storage capacity requirement, which are the two major areas of concern in numerical methods such as the finite difference and finite element methods.

Figure 3 depicts the comparison of the present results with Chamberlain's air data (Chamberlain, 1983) for the range $10.4 \leq Ra_D \leq 5.05 \times 10^6$. It is found that the present results constantly lie below the experimental data; however for $Ra_D < 10^3$, the computed values are within the experimental error bounds, which are $\pm 3\%$ at $Ra_D = 5.05 \times 10^6$ and $\pm 7\%$ at $Ra_D = 10.4$. Figure 4 shows good agreement between the computed surface-mean Nusselt numbers and the finite-difference results

of Farouk (1982) and the correlations of Raithby-Hollands (1975), Yuge (1960), Kyte et al. (1953) and Cliff et al. (1978) over a wide range of Rayleigh numbers. The general trend observed is that the computed values are lower than the data by the other authors, indicating a tendency for the present study to underestimate the surface-mean Nusselt number (particularly at high Ra_D). An indepth comparison of the present results with the data by the other authors is presented in tabular forms in the author's thesis (Lo Choy, 1988) and is summarized in Table 1.

The present results lie consistently below those predicted by the Raithby-Hollands correlation and were found to agree with the latter to within 10% for $Ra_D < 10^6$. Churchill's correlation for isothermal spheres (Churchill, 1983) was also considered. However, since Churchill's correlation is within 1.5% of Raithby-Hollands correlation for $Pr = 0.71$, the results will not be elaborated; the trend being the same as that observed with the latter. The best agreement is achieved with Yuge's correlation for the range of Rayleigh numbers within which the correlation is valid, i.e. $Ra_D < 10^5$. Comparison of the computed results with the two correlations of Kyte et al. shows the same trend observed with the Raithby-Hollands correlation at high Ra_D . This is due to the fact that at high Ra_D , the two aforementioned correlation equations predict values of the Nusselt number which are almost identical. As Ra_D decreases, the equation of Kyte et al. departs from the correlation of Raithby-Hollands to become in excellent agreement with the present results. A maximum error of 13.4% is observed with Kyte's correlations at $Ra_D = 10^7$; however, agreement is within 4% over the range $Ra_D < 10^4$. Figure 5 compares the local Nusselt number distribution of the present study for $Ra_D = 10^6$ with Churchill's correlation for isothermal spheres (Churchill, 1983). Good agreement is observed for $\theta \leq 150^\circ$, where the percentage difference is within 10%. At $\theta > 150^\circ$, the two sets of data diverge significantly from each other; however, this large difference has little effect on the surface-mean Nusselt number due to the relatively small surface area available for heat transfer in this region. In the region that controls the surface-mean Nusselt number, i.e. in the vicinity of $\theta = 90^\circ$, excellent agreement is observed between the present results and Churchill's correlation.

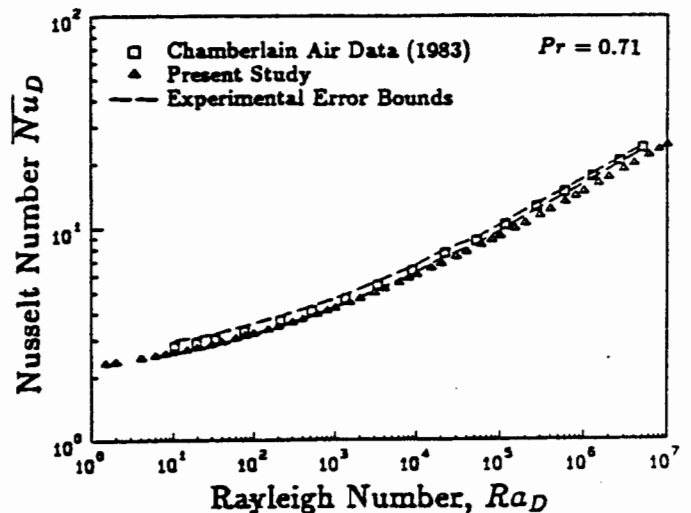


Figure 3: Comparison of present results with the air data of Chamberlain (1983)

Table 1: Comparison of present results with the available data from different sources

Author	Range of Ra_D	rms percent difference	max. percent difference
Kyte et al. (1953)	$1.5 - 1.0 \times 10^7$	6.68	13.40
Yuge (1960)	$1.5 - 1.0 \times 10^5$	4.03	5.98
Raithby-Hollands (1975)	$1.5 - 1.0 \times 10^7$	8.00	13.37
Cliff et al. (1978)	$1.5 - 1.0 \times 10^7$	4.95	9.31
Farouk (1982)	$1.5 - 1.0 \times 10^5$	5.18	7.18
Chamberlain (1983)	$10.4 - 5.05 \times 10^6$	7.76	11.14

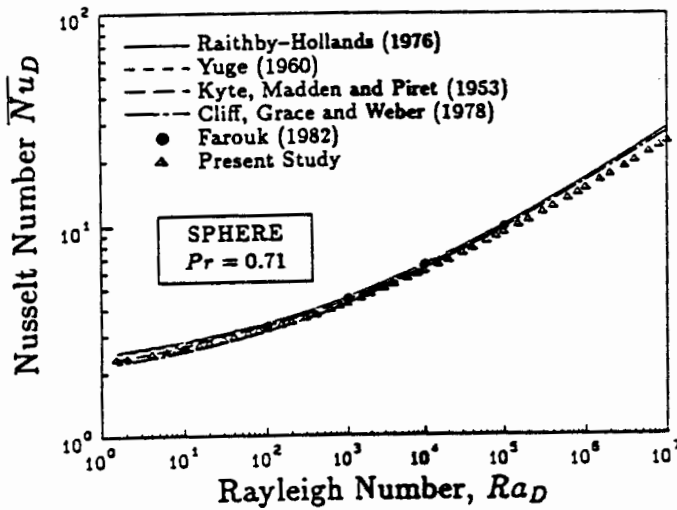


Figure 4: Comparison of present results with data from different sources

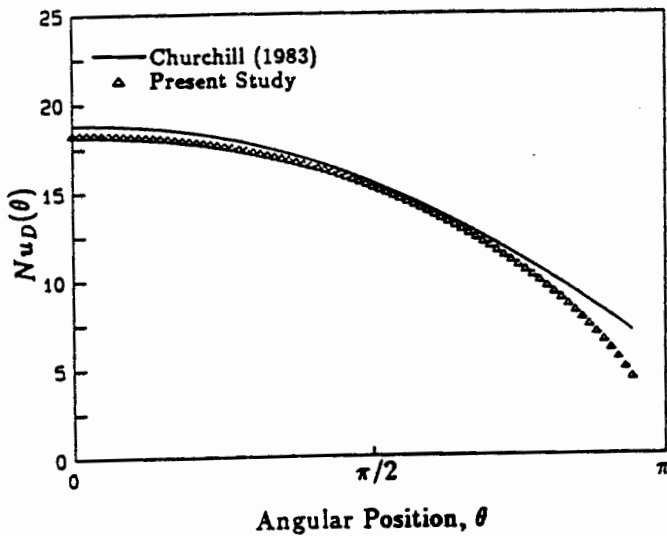


Figure 5: Local Nusselt number distribution at $Ra_D = 10^6$

In view of the reasonably accurate results obtained herein over a wide range of Rayleigh numbers, it can be concluded that the present study is very promising and enables fast computation of heat transfer data with accuracy that is sufficient for most engineering purposes. The increasing departure of the computed surface-mean Nusselt numbers from data by other authors at high Ra_D may also be related to the failure of the assumed temperature profile to approximate the actual profile at high Ra_D . In fact, it was brought to the attention of the reader earlier that the assumed temperature profile, derived from Laplace's equation for pure radial conduction, does not approximate the condition of negligible interfacial heat transfer at the edge of the thermal boundary layer for high Rayleigh numbers. Moreover, at high Rayleigh numbers, the temperature profile approaches a linear distribution; this being related to the fact that the solution of Laplace's equation in spherical coordinates approaches the solution for a flat plate in cartesian coordinates when the thermal boundary layer becomes very thin. The present integral approach is attractive from a mathematical point of view in that no specific mathematical skills are required for a good understanding and appreciation of the analysis; knowledge of basic integration and differentiation is adequate. The simplicity of its formulation, the small computational time and its good accuracy over a wide range of Rayleigh numbers are the main justifications of the present study.

ACKNOWLEDGEMENTS

The authors acknowledge the financial support of Natural Sciences and Engineering Research Council under the operating Grant A7445 for Dr. Yovanovich.

REFERENCES

- Amato, W.S. and Tien, C., 1972, "Free Convection Heat Transfer From Isothermal Spheres in Water," *Int. J. Heat Mass Transfer*, Vol. 15, pp. 307-339.
- Chamberlain, M.J., 1983, *Free Convection Heat Transfer From a Sphere, Cube and Vertically Aligned Bisphere*, M.A.Sc. Thesis, Department of Mechanical Engineering, University of Waterloo.

Cheney, W., and Kincaid, D., 1985, *Numerical Mathematics and Computing*, 2nd ed., Brooks/Cole Publishing Company, Monterey, California, p. 394.

Chiang, T., Ossin, A., and Tien, C.L., 1964, "Laminar Free Convection from a Sphere," *Trans. ASME, Series C*, Vol. 86, No. 4, pp. 537-542.

Churchill, S.W., 1983, "Comprehensive, Theoretically Based Correlating Equations for Free Convection From Isothermal Spheres," *Chem. Eng. Commun.*, Vol. 24, Gordon and Breach, Science Publishers, Inc., pp. 339-352.

Cliff, R., Grace, J.R., and Weber, M.E., 1978, *Bubbles, Drops and Particles*, Academic Press, New York, pp. 251-254.

Farouk, B., 1982, "Natural Convection Heat Transfer From an Isothermal Sphere," Proc. 16th Southeastern Seminar on Thermal Sciences, Miami.

Geoola, F., and Cornish, A.R.H., 1981, "Numerical Solution of Steady-State Free Convection Heat Transfer from a Solid Sphere," *Int. J. of Heat and Mass Transfer*, Vol. 24, No. 8, pp. 1369-1379.

Hossain, M.A., and Gebhart, B., 1970, "Natural Convection About a Sphere at Low Grashof Number," *Heat Transfer 1970*, Vol. IV, NC1.6, Elsevier Publishing Company, Amsterdam.

Hughes, W.F., and Gaylord, E.W., 1964, *Basic Equations of Engineering Science*, Schaum publishing company, New York.

Incropera, F.P., and DeWitt, D.P., 1985, *Fundamentals of Heat and Mass Transfer*, 2nd ed., Wiley, New York.

Jaluria, Y., 1980, *Natural Convection Heat and Mass Transfer*, Pergamon Press, U.K.

Kyte, J.R., Madden, A.J., and Piret, E.L., 1953, "Natural Convection Heat Transfer at Reduced Pressure," *Chemical Engineering Progress*, Vol. 49, pp. 653-662.

Levy, S., 1955, "Integral Methods in Natural Convection Flow," *J. Appl. Mech.*, pp. 315-322.

Lo Choy, C.C., 1988, *Approximate Methods for Solving Forced and Free Convection Heat Transfer from Isothermal Spheroids*, M.A.Sc. Thesis, Department of Mechanical Engineering, University of Waterloo.

Merk, H.J., and Prins, J.A., 1953-1954, "Thermal Convection in Laminar Boundary Layers," I, II, III, *Applied Scientific Research*, sec. A, Vol. 4, pp. 11-24, 195-206, 207-224.

Peterka, J.A., and Richardson, P.D., 1969, "Natural Convection From a Horizontal Cylinder at Moderate Grashof Numbers," *Int. J. of Heat and Mass Transfer*, *TRANS. ASME, Series C*, Vol. 12, pp. 749-752.

Raithby, G.D., and Hollands, K.G.T., 1973, "A General Method of Obtaining Approximate Solutions to Laminar and Turbulent Free Convection Problems," *Advances in Heat Transfer*, Academic Press, Vol. 11, pp. 267-315.

Yovanovich, M.M., 1987, "New Nusselt and Sherwood Numbers for Arbitrary Isopotential Bodies at near Zero Peclet and Rayleigh Numbers," Paper AIAA- 87-1643, AIAA 22nd Thermophysics Conference, Honolulu, Hawaii, June 8-10, 1987.

Yuge, T., 1960, "Experiments on Heat Transfer from Spheres including Combined Natural and Forced Convection," *Trans. ASME, Series C*, Vol. 82, pp. 214-220.

M. Yovanovitch
890308

HTD-Vol. 110

NUMERICAL HEAT TRANSFER WITH PERSONAL COMPUTERS AND SUPERCOMPUTING

presented at
THE 1989 NATIONAL HEAT TRANSFER CONFERENCE
PHILADELPHIA, PENNSYLVANIA
AUGUST 6-9, 1989

sponsored by
THE HEAT TRANSFER DIVISION

edited by
R. K. SHAH
GENERAL MOTORS CORPORATION

CONTENTS

NUMERICAL HEAT TRANSFER WITH PERSONAL COMPUTERS

Analytical/Numerical Solution of Convective Heat Transfer in the Thermal Entrance Region of Irregular Ducts <i>H. Y. Zhang, A. Campo, and M. A. Ebdian</i>	1
Effects of Heat Generation and Axial Heat Conduction in Laminar Flow Inside a Circular Pipe With a Step Change in Wall Temperature <i>H. Y. Zhang, M. A. Ebdian, and A. Campo</i>	9
A Suite of Personal Computer Programs for Undergraduate Education in the Thermal Sciences <i>B. K. Hodge</i>	19
A Generalized Program for Computing Two-Dimensional Boundary Layers on a Personal Computer <i>B. Gatlin and B. K. Hodge</i>	25
Microcomputer Software for Heat Transfer Education <i>S. V. Patankar and K. M. Kelkar</i>	31
Modeling of Strip Cooling Using Finite Difference and Finite Element Methods With an IBM PC/AT <i>S.-J. Chen, K. Sadeghipour, and F. Han</i>	35
Finite Difference Model for Heat Transfer in a Stratified Thermal Storage Tank With Throughflow <i>C. R. Truman and M. W. Wildin</i>	45
PC-Based Adaptive Irregular Triangular Grid Generation for Transient Diffusion Problems <i>J. H. Kim, C. W. Meyers, and P. V. Desai</i>	57
Numerical Generation of Orthogonal Boundary-Fitted Grids for Heat and Fluid Flow <i>M. Wang and J. G. Georgiadis</i>	65
Numerical Studies of Convective Heat Transfer in an Inclined Semi-Annular Enclosure <i>L.-W. Wang, C.-N. Yung, A.-T. Chai, and N. Rashidnia</i>	73
An Application of Boundary Element Methods to a Transient Axisymmetric Heat Conduction Problem <i>F. Kavoosi, M. di Marzo, H. R. Baum, and D. D. Evans</i>	79
Microcomputer Computation of Natural Convection Heat Transfer From Isothermal Spheres Into Air for Rayleigh Numbers From 1.5 to 10^7 <i>C. C. Lo Choy and M. M. Yovanovich</i>	87
Capabilities of Personal Computers for Numerical Convective Heat Transfer <i>L. S. Caretto and A. K. Runchal</i>	95
One-Dimensional Analysis of Plane and Radial Thin Film Flows Including Solid-Body Rotation <i>S. Thomas, W. Hankey, A. Faghri, and T. Swanson</i>	103
Analysis of the Transient Compressible Vapor Flow in Heat Pipes <i>J. H. Jang, A. Faghri, and W. S. Chang</i>	113
Transient Combined Mixed Convection and Radiation From a Straight Vertical Fin <i>P. S. Ghoshdastidar and Y. S. T. Raju</i>	121
Mold-Cooling Simulation in Injection Molding of Three-Dimensional Thin Plastic Parts <i>K. Himasekhar, K. K. Wang, and J. Lottey</i>	129
A Finite Element Method for Fluid Flow and Heat Transfer on the Personal Computer <i>D. W. Pepper and A. P. Singer</i>	137
The Use of Finite Elements and PCs in Teaching Heat Transfer <i>A. F. Emery and A. Abrous</i>	147

SUPERCOMPUTING IN HEAT TRANSFER

Experience With the Application of Supercomputers to Computational Heat Transfer <i>K. A. Cliffe, J. R. Kightley, R. D. Lonsdale, C. P. Jackson, and I. P. Jones</i>	155
---	-----

Heat Transfer to a Thin Liquid Film With a Free Surface <i>M. M. Rahman, A. Faghri, W. L. Hankey, and T. D. Swanson</i>	161
Numerical Simulation of Internal Supersonic Flow <i>P. K. Russell and D. W. Pepper</i>	169
Spectral Element Simulations of Forced Convective Heat Transfer: Application to Supercritical Slotted Channel Flows <i>C. H. Amon and B. B. Mikic</i>	175
Numerical Prediction of Vortex Shedding Behind a Square Cylinder <i>K. M. Kelkar and S. V. Patankar</i>	185
A Preliminary Comparison of the $k-\epsilon$ and Algebraic Stress Models for Turbulent Heat Transfer in a Square Enclosure <i>D. J. Silva and A. F. Emery</i>	193